J Solid State Electrochem (2005) 9: 797–808
DOI 10.1007/s10008-005-0699-x

REVIEW

Trevor J. Davies · Craig E. Banks · Richard G. Compton

Voltammetry at spatially heterogeneous electrodes

Received: 19 April 2005 / Accepted: 25 April 2005 / Published online: 1 June 2005

Abstract Recent advances are overviewed which enable simulation of the voltammetric behaviour of surfaces which respond in an electrochemically spatially heterogeneous fashion. By use of the concept of a ''diffusion domain'' computationally expensive three-dimensional simulations may be reduced to tractable two-dimensional equivalents. In this way the electrochemical response of partially blocked electrodes and microelectrode arrays may be predicted, and are found to be consistent with experimental data. It is, furthermore, possible to adapt the ''blocked'' electrode analysis to enable the voltammetric sizing of inert particles present on an electrode surface. Finally theory of this type predicts the voltammetric behaviour of electrochemically heterogeneous electrodes—for example composites whose different spatial zones display contrasting electrochemical behaviour toward the same redox couple.

Keywords Heterogeneous electrodes · Cyclic voltammetry · Diffusion domain approximation · Microelectrode arrays · Partially blocked electrodes

Introduction

Electrodes which are spatially heterogeneous in the electrochemical sense embrace porous electrodes, partially blocked electrodes, microelectrode arrays, electrodes made of composite materials, and some modified electrodes [1, 2, 3, 4]. The simulation of electrode responses at such surfaces is challenging both because of the surface variation and because of the often random distribution of the zones of different electrode activity.

Recent simulation advances suggest that the use of the diffusion domain approach enables reduction of these complex three-dimensional problems to a readily tractable two-dimensional form which gives results in excellent agreement with experiment. The purposes of this paper are to overview these advances and illustrate the progress made.

T. J. Davies · C. E. Banks · R. G. Compton (✉)
Physical and Theoretical Chemistry Laboratory,
University of Oxford, South Parks Road,
Oxford, OX1 3QX, UK
E-mail: richard.compton@chem.ox.ac.uk
Tel.: +44-1865-275413
Fax: +44-1865-275410

Partially blocked electrodes

Figure 1 illustrates the concept of a partially blocked electrode. It shows four macro electrodes partially covered with particles of material distinct from that of the underlying electrode material. In the following discussion these particles are first assumed to be inert, so that they partially block the electrode towards electrolytic reactions. Subsequently they take the form of either electro-active particles on an inert substrate, as in a microdisc array or a nano-particle-modified electrode. As Fig. 1 implies, the particles, be they inert or electroactive, may take a variety of possible shapes. We have identified the voltammetric conditions under which this needs to be addressed in the modelling [3]; except where explicitly stated, the flat disc approximation was adopted (Fig. 1)

The diffusion domain approximation and partially blocked electrodes

Figure 2 shows an array of electrically inert blocks supported on a flat electrochemically active substrate. The blocks are disc spaced and arranged in a cubic distribution. Subtly, Fig. 3 shows a similar array except that the blocks are now randomly distributed over the electrode surface. It is interesting to consider the voltammetric behaviour of the simple process

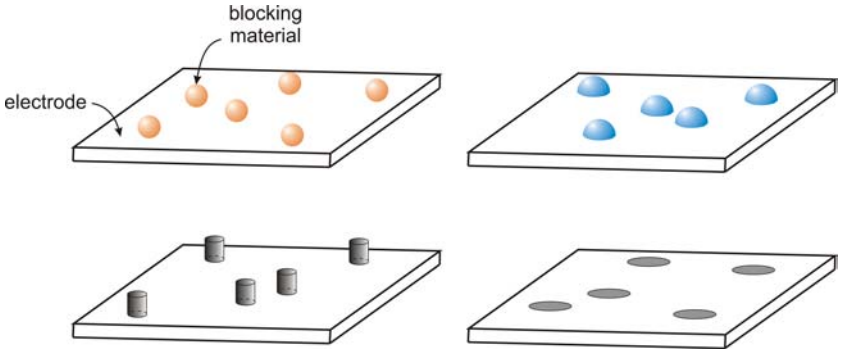

Fig. 1 Schematic representation of partially blocked electrodes shown for the case of spherical particles (*top left*), hemispheres (*top right*), cylinders (*bottom left*) and flat discs (*bottom right*)

$$A + e^- \underset{k_b}{\overset{k_l}{\rightleftarrows}} B$$

at such partially blocked electrodes, assuming that the dynamics follow Butler–Volmer kinetics so that:

$$k_a = k_o \exp\left(\frac{\beta F}{RT}\eta\right) \tag{1}$$

and

$$k_c = k_o \exp\left(-\frac{\alpha F}{RT}\eta\right) \tag{2}$$

where k_o is the standard electrochemical rate constant, α and β are transfer coefficients such that $\alpha + \beta = 1$, and η is the overpotential defined as:

$$\eta = E - E^{o'}_{A/B} \tag{3}$$

where E is the electrode potential and $E^{o'}_{A/B}$ the formal potential for the A/B couple.

The cyclic voltammetry response can be discovered [1, 2, 3, 4] by solving the transport equations:

$$\frac{\partial[A]}{\partial t} = D_A \nabla^2[A] \tag{4}$$

and

$$\frac{\partial[B]}{\partial t} = D_B \nabla^2[B] \tag{5}$$

subject to applying Eqs. (1), (2) and (3) as boundary conditions where the equations:

$$E = E_{start} + \upsilon t \quad 0 < t < \frac{E_{end} - E_{start}}{\upsilon} \tag{6}$$

at

$$E = E_{end} - \upsilon\left[t - \frac{(E_{end} - E_{start})}{\upsilon}\right] \tag{7}$$

define the potential sweep between E_{start} and E_{end} with a voltage sweep rate of υ V s^{-1} and D_A and D_B are the diffusion coefficients of A and B, respectively.

The above problem is posed in three spatial dimensions (x, y, and z or their equivalents). Accordingly the

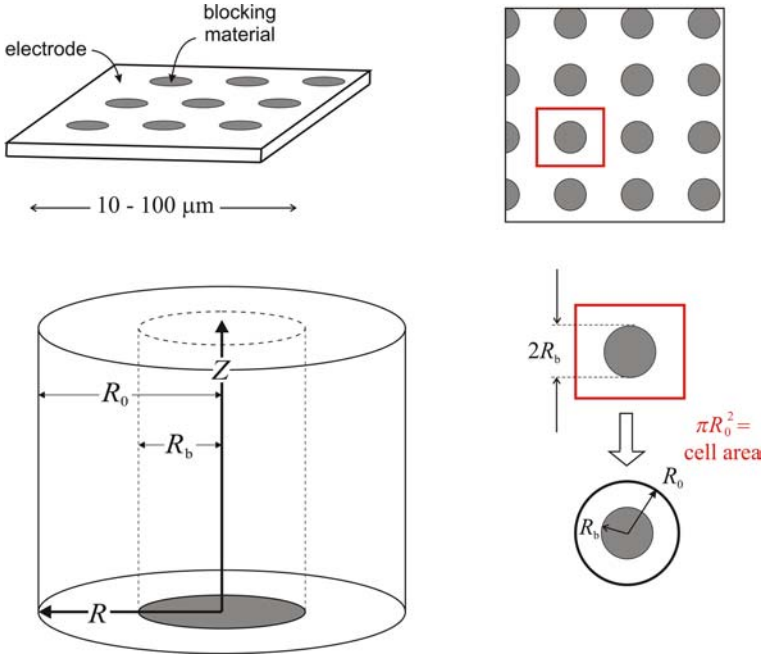

Fig. 2 The diffusion domain problem for electrically inert blocks in a cubically spaced distribution

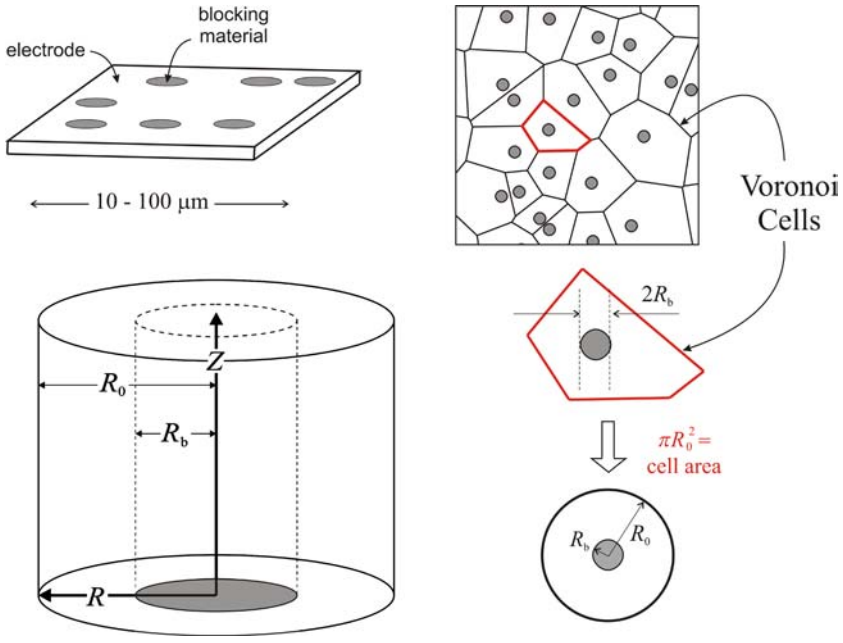

Fig. 3 Illustration of blocking material randomly distributed over an electrode surface, and the construction of Voronoi cells

solution for regularly distributed blocks is computationally expensive and that for the random distribution is essentially intractable. Accordingly we introduce the diffusion domain approximation.

Figures 2 and 3 illustrate the diffusion domain approximation for cubic and random arrays respectively. In Fig. 2 it can be seen that the electrode surface is first split into unit square cells each of the same area. The diffusion domain approximation involves replacing this by a circular domain to equal total area. Thus if the radius of the circular domain is R_0, then:

$$p^2 = \pi R_o^2$$

where p is the centre-to-centre distance between adjacent blocks or, equally, the length of the side of the square unit cell. Accordingly:

$$R_o = 0.564p$$

similarly, for a hexagonal area of blocks,

$$R_o = 0.5258p$$

Having made this approximation the diffusion equations, Eqs. (4) and (5), are solved within the cylindrical unit shown in Fig. 2 where Z is the direction normal to the electrode surface and R is the radial coordinate with R_0 defining the radius of the cylinder and R_b the size of the block. Within this approximation Eqs. (4) and (5) become:

$$\frac{\partial[\mathrm{A}]}{\partial t} = D_\mathrm{A}\frac{\partial^2[\mathrm{A}]}{\partial r^2} + \frac{D_\mathrm{A}}{r}\frac{\partial[\mathrm{A}]}{\partial r} + D_\mathrm{A}\frac{\partial^2[\mathrm{A}]}{\partial z^2} \tag{8}$$

and

$$\frac{\partial[\mathrm{B}]}{\partial t} = D_\mathrm{B}\frac{\partial^2[\mathrm{B}]}{\partial r^2} + \frac{D_\mathrm{B}}{r}\frac{\partial[\mathrm{B}]}{\partial r} + D_\mathrm{B}\frac{\partial^2[\mathrm{B}]}{\partial z^2} \tag{9}$$

and the three dimensional problem is accordingly transformed into a tractable two dimensional equivalent. In solving, the boundary conditions of "no flux" are imposed on the walls of the cylinder so that each cylinder is diffusionally independent of it neighbours and the response of the macroelectrode as a whole is simply that one single diffusion domain multiplied by the total number of blocks on the electrode surface. Figure 3 shows the diffusion domain approximation in respect of the randomly distributed blocks in the shape of discs. Here the surface is first decomposed into a set of Voronoi cells. These are defined as follows. Treat each N disks present as a point located at the centre of the disk. Locate the nearest neighbour of every point and divide the distance between each set of neighbours in half. Voronoi cells in the shape of polygons are then formed by linking together all the "halfway" points surrounding a particular disc. Each disc then occupies its own Voronoi cell of area A_n where n represents the number assigned to the particles ($n = 1,2...N-1, N$) and the total area of the electrode, A_{elec} is given by a sum over the N cells present:

$$A_{\mathrm{elec}} = \sum_{n=1}^{N} A_n \tag{10}$$

Now consider the walls of a particular unit (Voronoi) cell. Because the walls are equidistant from the surrounding blocks, the environment on both sides of each wall will be similar. Thus, little or zero net flux of species A (or B) will pass through the cell walls. This means that each cell can be considered diffusionally independent and to simulate the voltammogram of a modified electrode we simply sum the voltammograms of every unit cell on the electrode surface. A Voronoi cell is, however, an awkward and irregular shape to simulate, so we again

make use of the *diffusion domain approximation*: we approximate the base of each Voronoi cell as a circle of the same area containing the same block (Fig. 3). As illustrated in Fig. 3, this results in a cylindrical unit cell (a diffusion domain) with radius R_0, which is much easier to simulate. An important property of diffusion domains is the microscopic coverage, θ, given by Eq. (11):

$$\theta = \frac{\pi R_b^2}{\pi R_0^2} = \left(\frac{R_b}{R_0}\right)^2 \tag{11}$$

where θ is the block coverage [1, 2, 3, 4].

Simulation of the cyclic voltammetry problem for the random distributed partially blocked electrode then involves solving Eqs. (8) and (9) as above but for a range of R_0 values. In the case of randomly distributed blocks the nearest neighbours show a Poisson distribution:

$$P(R_o) = \frac{2\pi R_o N}{A_{elec}} \exp\left(\frac{-\pi R_o^2 N}{A_{elec}}\right) \tag{12}$$

where the probability of finding domains of radius R_0 is given by P(R_0) and the probability of finding domains of radius $R_0 + \mathrm{d}\ R_0$ is given by P(R_0)d R_0 . The cyclic voltammograms calculated for different R_0 must be weighted accordingly to produce the final voltammogram; Fig. 4 shows the procedure.

The results of the simulation can be illustrated with reference to the following "thought experiment". We consider a naked macroelectrode, say of dimension 4 mm × 4 mm, and explore the cyclic voltammetric response resulting from an A/B couple with "typical" aqueous solution properties $\alpha = 0.5$, $k_o = 10^{-2}$ cm s^{-1} and $D_A = D_B = 10^{-5}$ cm^2 s^{-1}. We assume a voltage scan rate of $\upsilon = 0.01$ V s^{-1}. The expected voltammogram is shown in Fig. 5 for a completely unblocked electrode.

We next pose the question: what does the voltammogram look like if the electrode is 50% blocked? In particular we consider the responses when the blocks are of different size but in each case the total block coverage is $\theta = 0.5$. Figure 5 illustrates these three results—first when the electrode has a single macro-block of $R_0 = 0.18$ cm ($\pi \times 0.18^2 = 0.5 \times 0.4 \times 0.4$), second when the electrode is covered with 50 μm radius blocks spread 200 μm apart in a cubic array, and third when the electrode is half covered with 1 μm radius blocks. The different cyclic voltammetric responses are shown in Fig. 5. It can be seen that the single macro-block ($R_0 = 0.18$ cm) produces a voltammetric response that is close to giving just one half the current of the unblocked electrode. In contrast the effect of blocking the electrode with many 1 μm blocks is tiny; the voltammogram is only slightly reduced in magnitude in comparison with the unblocked electrode. The voltammetry seen with the electrode blocked by 50 μm lies intermediate between the unblocked and the macroscopically blocked case.

The reason for the contrasting behaviour can be seen from the consideration of the concentration profiles of A with the different diffusion domain of the three examples. These are shown in Fig. 6. For the single block there is "linear" diffusion to the active part of the electrode whilst the concentration of A remains close to its bulk value over the zone of the block. For the 50-μm blocks the "linear" diffusion to the active electrode is augmented by significant radial diffusion that is sufficient to reduce, but not exhaust, the amount of A in the block zone. Finally for the 1-μm blocks the radial diffusion is enough to enable the near complete electrolysis of all A arriving at the electrode so that the partially blocked electrode behaves almost like an unblocked electrode even though 50% of its surface is not active!

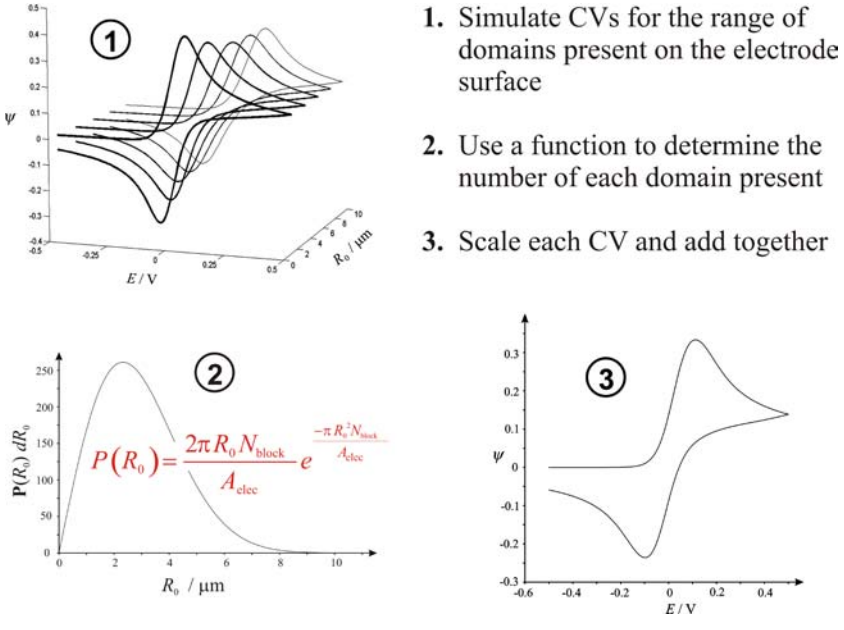

Fig. 4 Illustration of the steps involved in the simulation of cyclic voltammograms for a random ensemble of diffusion domains

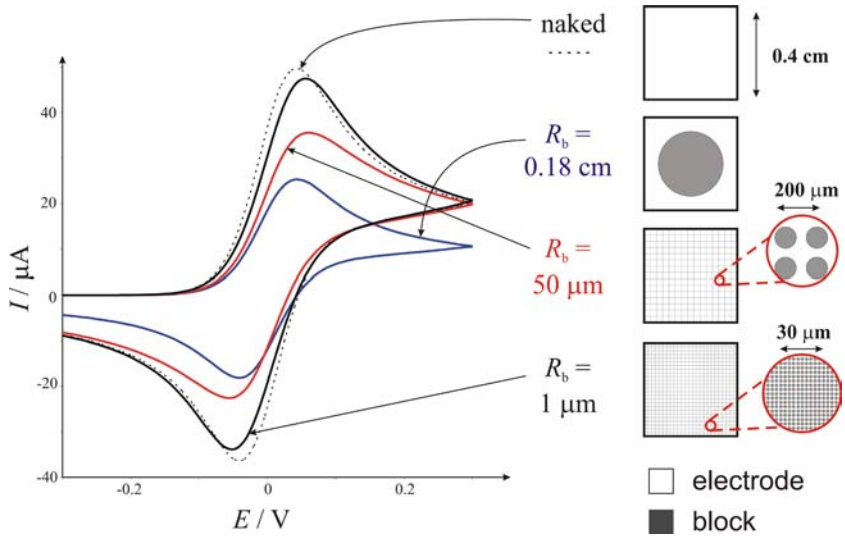

Fig. 5 The expected voltammetric responses for different sized blocks each corresponding to a total coverage of $\theta = 0.5$

It is clear that the voltammograms in Fig. 5 cover a range of voltammetric behaviour for a heterogeneous electrode part of which is active and part inert. In fact four categories of response can be defined and these are illustrated in Fig. 7. We next discuss each category in turn.

Case 1

In this limit both the blocked and unblocked surface are macroscopically "large". Accordingly the unblocked electrode experiences linear diffusion, as at an ordinary electrode of the same active dimension, whilst the concentration of the electro-active species in the vicinity of the block is essentially unchanged from that of the bulk solution. In this limit the voltammogram observed is simply the same as that measured for an unblocked electrode of the same size except that the current scale is reduced by the factor $(1-\theta)$.

Case 2

In this case the size of the electro-active zones are "micro" in size but are separated with sufficiently large inert blocking material such that the electrode as a whole behaves as a collection of isolated microelectrodes, each of which experiences convergent diffusion (radial and axial) as illustrated in Fig. 7.

Case 3

In this situation the electro-active parts of the macroelectrode behave with "microelectrode" character; their

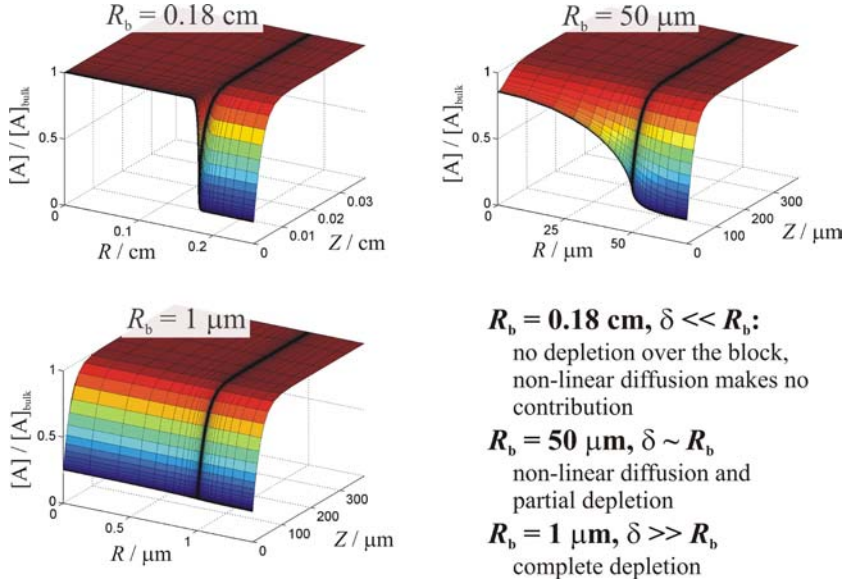

Fig. 6 Concentration profiles of A within different diffusion domains

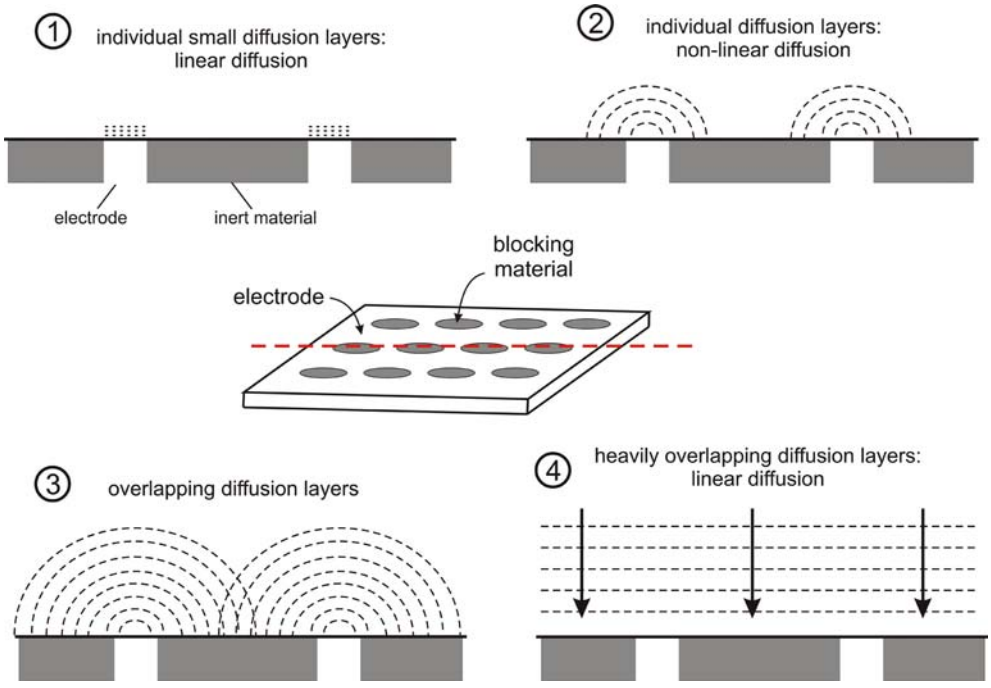

Fig. 7 Voltammetric behavior for a heterogeneous electrode with active and inert parts, illustrating Cases 1, 2, 3, and 4. (see text)

size is such that a convergent diffusion regime is established, as in Case 2. However, in Case 3 the scale of the insulating parts of the electrode is sufficiently small that the diffusion fields of adjacent electro-active zones begin to overlap. This case is illustrated by the example of the 50-μm blocks on the 4-mm^2 electrode discussed above.

Case 4

This represents the limiting situation of Case 3 where the diffusion field of the electro-active "microelectrode"-sized zones overlap so heavily that the heterogeneous electrode as a whole behaves almost like an unblocked electrode. This situation corresponds to the example of the 1-μm blocks on the 4 mm^2 electrode investigated above. This limiting case has previously been explained by Amatore [5] who concluded, and this is now verified by our simulations [1, 2, 3, 4], that the electrode response is exactly that of the unblocked electrode but calculated for an electrochemical rate constant of $(1-\theta)$ multiplied by k_o. In other words redox couples with a Butler–Volmer rate constant of k_o have linear diffusion characteristics at a partially blocked electrode of coverage θ but with an *apparently* reduced electrochemical rate constant of k_o $(1-\theta)$.

In summary Case 1 and Case 4 limits both show the characteristics of linear diffusion and as such will generate votlammograms that can be fitted using commercial simulation programs such as Digisim which apply one-dimensional diffusion models only. Case 2 presents the case where the electrode responds as an array of diffusionally independent microelectrodes. Last, Case 3 is interesting since it generates voltammograms which *can never* be simulated on the basis of linear diffusion, e.g. via Digisim. Figure 8 illustrates an attempt to model a simulated Case 3 voltammogram using Digisim; the figure shows the best fit to the forward peak. It is clear that the Digisim modelling is inadequate for the whole voltammogram; the reverse peak is too big and the forward going diffusional tail falls off too quickly. Both features are indicative of vestigial microelectrode voltammetric characteristics almost, but not fully, lost

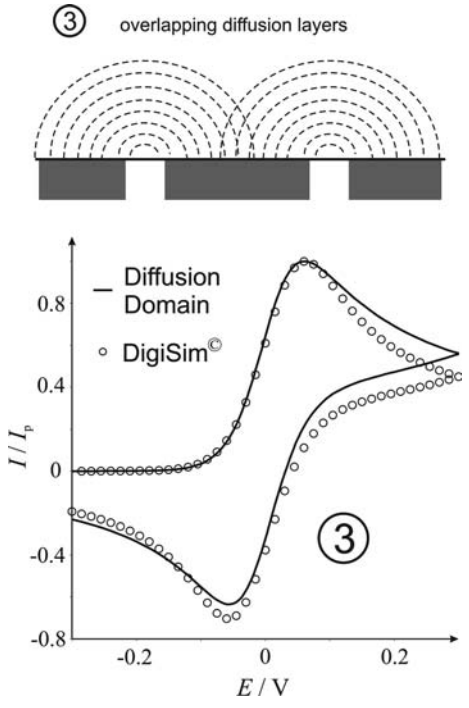

Fig. 8 Attempt to model a Case 3 voltammogram using Digisim

through the overlapping of adjacent microelectrode diffusional fields.

How big is "big" and how small is "small"? The Einstein equation provides the answer

In our above analysis of partially blocked electrodes the difference between macroelectrodes and microelectrodes, between "big" and "small", was critical. How can we tell whether the dimensions of the electro-active or inert zones of heterogeneous electrodes fall into one category or another (Cases 1, 2, 3 or 4)? Without recourse to simulation we can answer we such question using the Einstein equation [6].

The Einstein equation indicates that the approximate distance, δ, diffused by a species with a diffusion coefficient, D, in a time, t, is:

$$\delta = \sqrt{2Dt} \tag{13}$$

In considering the cyclic voltammetry problem above we can estimate the appropriate value of t, by considering the appropriate potential "width" of the voltammogram, ΔE so that:

$$\delta = \sqrt{2D\frac{\Delta E}{\upsilon}} \tag{14}$$

for a typical nearly "reversible" voltammogram a ΔE of the order 0.1 to 0.15 V, as illustrated in Fig. 9. Accordingly if we return to the concentration profiles reported in Fig. 6, using the parameters adapted in the simulations and a value of ΔE of 0.15 V we can estimate that:

$\delta \approx 55\ \mu$m

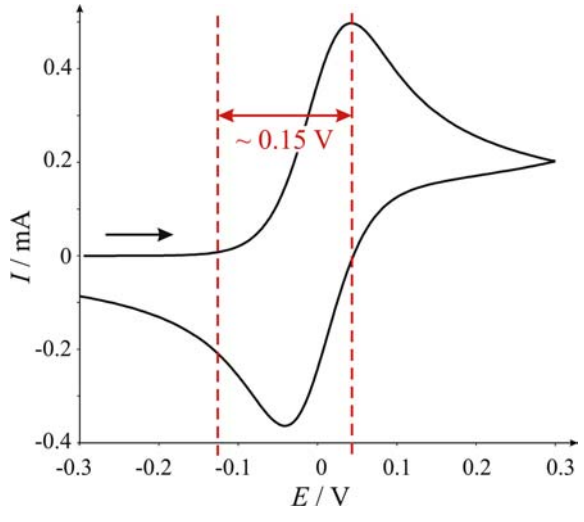

Fig. 9 The potential "width" of a voltammogram

It can be seen that this approximately corresponds to the thickness of the diffusion layer associated with the linear diffusion part of the macroelectrode partially blocked with the single 0.18 cm "macro block" in Fig. 6 (Case 1) and to that in the heavily overlapping diffusion case for the 1-μm blocks (Case 4). On the other hand, this value of δ roughly corresponds to the size of the blocks in the case they were assumed to be of 50 μm radius. Accordingly in this last case Fig. 6 shows significant diffusional depletion over the block in this case. It follows that simply using Eq. (14) to estimate the diffusional distance, and noting that this is comparable with the block size, immediately indicates that cyclic voltammetry conducted at 0.1 V s^{-1} (as used to generate Fig. 6) will fall into Class 3. As such it will not be accurately modelled by assuming linear diffusion (as, for example, via Digisim).

In conclusion, use of Eq. (14) permits the determination of Classes 1, 2, 3 and 4 for partially blocked electrodes; the Einstein equation generates values of δ which "benchmark" whether the electrodes and blocks are "big" or "small" compared with diffusion layer thicknesses.

Partially blocked electrodes: results

To test the theory above we lithographically constructed partially blocked electrodes comprising macroelectrodes partially covered with inert discs of a fixed size arranged in either a cubic or hexagonal array [1, 2]. Electrodes with different coverage and different radii were constructed with gold as the electrode material. The oxidation of 1,4-*N,N,N′,N′*-tetramethylphenylenediamine (TMPD) in acetonitrile was studied as a function of voltage scan rate with the peak current measured. Excellent agreement between theory and experiment was noted [1, 2].

Next, partially blocked electrodes with *random* arrays of disc-shaped blocks were fabricated [2]; Fig. 10 shows a typical electrode. Again variable scan rate voltammetry with the TMPD–acetonitrile system was examined to verify the diffusion domain theory. Figure 11 shows the measured peak current as a function of the square root of the voltage scan rate, υ. The solid line shows the expected behaviour for an unblocked electrode; the points show excellent agreement between theory and experiment for the two different coverages (θ) of 0.1 and 0.5.

The above experiments serve to validate the diffusion domain approximation both in the context of regularly and randomly heterogeneous electrodes. We have therefore applied this approach more generally in a variety of contexts which we now briefly address.

Electrochemical particle sizing

Implicit in the discussion above is the notion that voltammetric measurements made on partially blocked

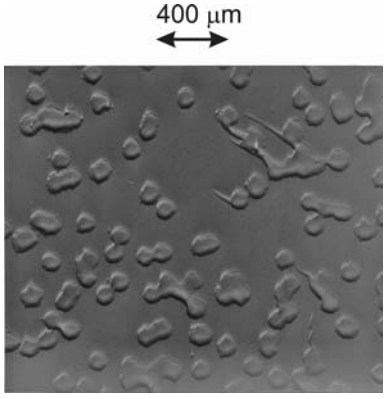

Fig. 10 A lithographically fabricated partially blocked electrode with random arrays of discs on the surface

electrode can give us information about the coverage or size of the material on the surface of an electrode. That is to say, that in principle, voltammetry has the capability for particle sizing [7].

To illustrate proof-of-concept we modified an edge-plane pyrolytic graphite electrode with known masses, m_{block}, of monodisperse (approximately spherical) particles of alumina of diameter 1 µm using the procedure outlined in Fig. 12. The aqueous ferricyanide/ferrocyanide redox couple was used for voltammetric measurements with these modified (blocked) electrodes and with the corresponding unblocked electrodes. Typical data are shown in Fig. 13; the effect of an increased mass of alumina particles on the electrode surface was to reduce the peak currents while slightly increasing the peak-to-peak voltage separation. The data were modelled assuming blocking by monodisperse inert spheres of radius R_b. For a given radius the number of blocking particle was calculated as:

$$N_{\text{block}} = \frac{3m_{\text{block}}}{4\rho\pi R_b^3} \tag{15}$$

where ρ is the density of the alumina. Figure 14 shows a comparison of experiment and theory generated for different values of R_b. Almost perfect fit is seen for

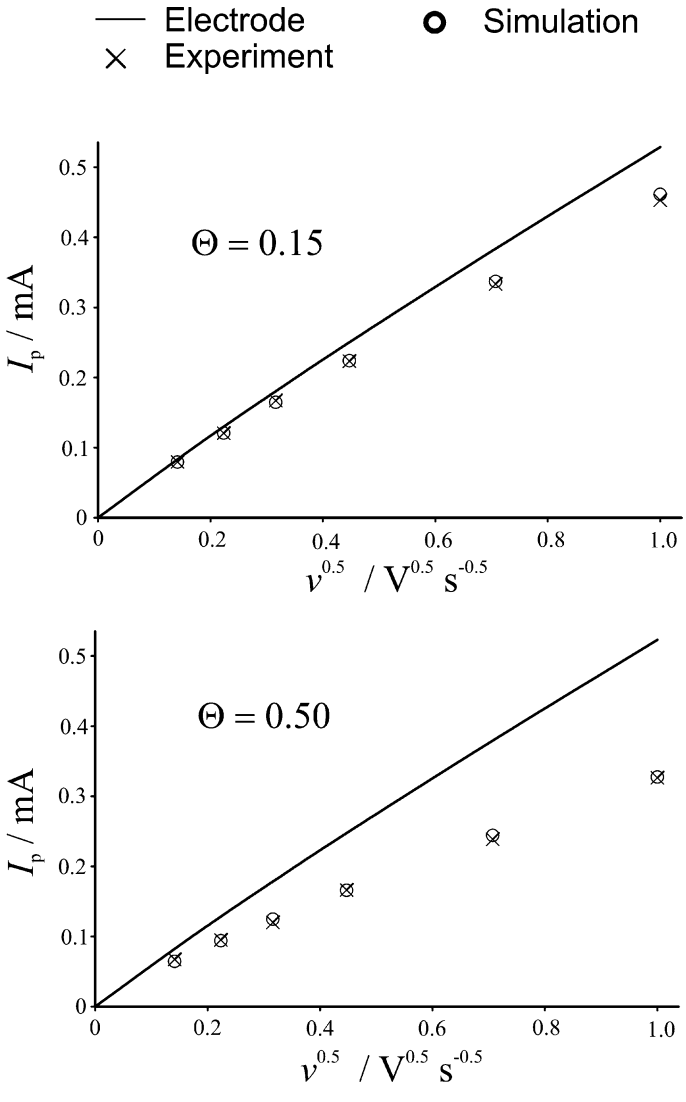

Fig. 11 The measured peak current as a function of the square root of the voltage scan rate, υ, using the experimental system of TMPD in acetonitrile to verify the diffusion domain theory

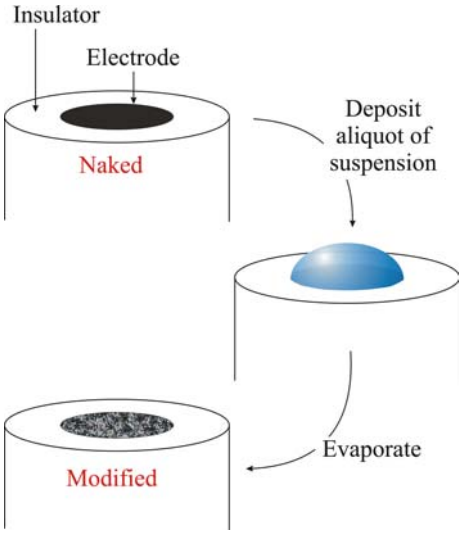

Fig. 12 Procedure for modifying an edge-plane pyrolytic-graphite electrode with a suspension containing alumina particles for voltammetric particle sizing

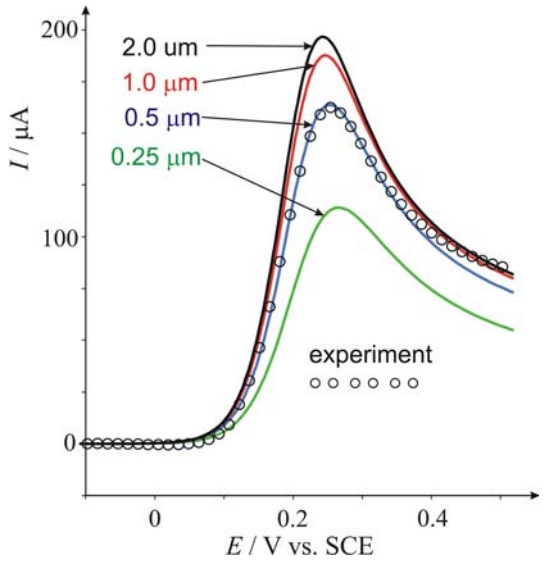

Fig. 14 Comparison of experiment with theory generated for different values of R_b

$R_b = 0.5$ μm corresponding to the known, independently established, diameter of 1 μm, confirming the scope of using voltammetry for particle sizing [7].

Another application in which we have used voltammetry to estimate the size of inert material on an electrode surface is for material on the surface of microdroplet-modified electrodes [3, 8, 9, 10, 11, 12, 13, 14, 15, 16]. Here water-insoluble oils form micron or larger sized droplets—typically on platinum or basal plane pyrolytic graphite electrodes; the latter are then immersed in aqueous electrolyte for voltammetry. These modified electrodes are important in that electro-generated species (formed at the unblocked part of the electrode) can react at the oil droplet and the kinetics and mechanism of this interfacial liquid–liquid process can be investigated. Similarly voltammetric monitoring of processes with the droplet is possible; for example photo-generated species can be detected [12, 13]. In both case knowledge of the droplet size is required for modelling and for extraction of quantitative kinetic data. This can be obtained by means of the methodology presented above; variable scan-rate voltammetry of stable, water-soluble redox species which are unreactive toward the oil droplet are used to provide good estimates of the sizes of the droplets, the latter acting as the inert blocks on the partially blocked electrode.

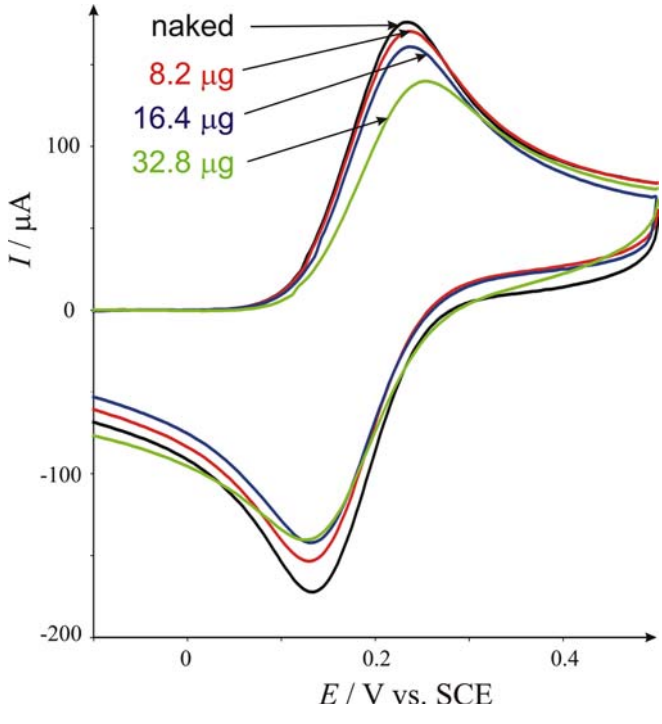

Fig. 13 The observed effect on the voltammetric response of increasing the mass of alumina on the voltammetric response

Microelectrode arrays

Microelectrode arrays are now widely used in electroanalysis [17]. Typically they comprise a regular array of microdisc electrodes separated from each other by a distance of ten or more diameters; if the latter separation if sufficiently large then each microdisc electrode behaves in a diffusionally independent manner and the total current response simply reflects that of a single microdisc multiplied by the number of electrodes present. On the other hand the merits of randomly distributed arrays for some applications have also been noted [18].

Simulation of microdisc arrays to address the key issue of diffusional independence can easily be achieved by means of an obvious modification of the theory

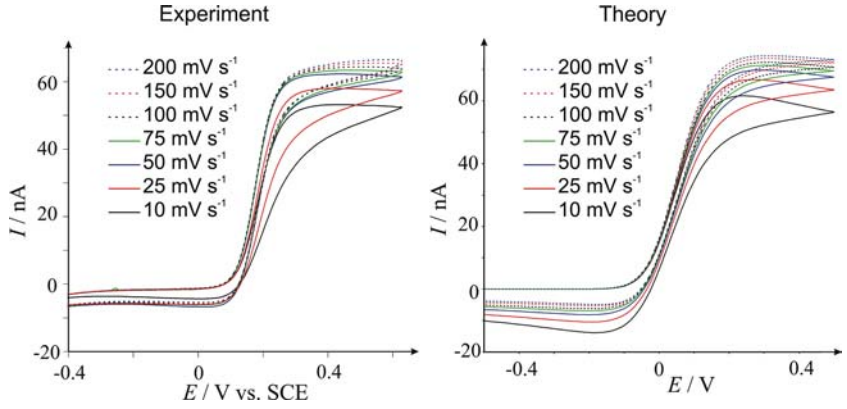

Fig. 15 The simulation of microdisc arrays addressing the issue of diffusional independence. Shown are experimental voltammetric results obtained from oxidation of 1 mmol L^{-1} ferrocyanide in 0.1 mol L^{-1} KCl at a gold microdisc array comprising a cubic distribution of 10-μm-diameter discs with centre-to centre nearest neighbour separations of 100 μm. Scan rates used (from *bottom* to *top* of the curves) were 10, 25, 50, 75, 100, 150, 200 mV s^{-1}

presented above. The results are in excellent agreement with experiment. For example, Fig. 15 shows experimental voltammetric results from oxidation of aqueous ferrocyanide, obtained at a gold microdisc array comprising a cubic distribution of 10-μm-diameter discs with centre-to centre nearest neighbour separations of 100 μm. The expected scan rate-independent sigmoidal current–voltage characteristics are seen at the higher scan rates but not below ca 50 mV s^{-1}. Also shown are the corresponding simulated voltammograms; excellent agreement between theory and experiment is apparent. Moreover we can understand the scan rate behaviour on the basis of Eq. (14). Noting that the block radius (R_b) in this case is 45 μm we can calculate that for scan rates of 10 and 25 mV s^{-1}, δ has values of 125 and 80 μm respectively, so for these scan rates the electrode is showing Case 3 behaviour. In contrast, for a scan rate of 100 mV s^{-1}, δ has the value of 40 μm, so this represents the onset of Case 2 behaviour which is followed at this scan rate and above.

Electrochemically heterogeneous electrodes

The simplest model of an electrochemically heterogeneous electrode (EHE) is shown schematically in Fig. 16. It is similar in concept to a partially blocked electrode except that rather than having inert and electro-active zones, in the EHE both types of zones are electro-active, albeit with different Butler–Volmer terms, $\{k_1^0, \alpha_1\}$ and $\{k_2^0, \alpha_2\}$. The simulation of such an electrode proceeds using the diffusional domain approach such as already explained. The power of the method can be illustrated with reference to an electrode comprising gold particles, of known average radius, abrasively attached [19, 20] to an edge-plane pyrolytic-graphite electrode which has been modified by physical adsorption of anthraquinone [3]. The effect of the adsorption is to slow the electron transfer kinetics of the edge-plane pyrolytic-graphite electrode in respect of the electro-oxidation of ferrocyanide; the standard rate constant is measured using a pure, unmodified electrode as 0.0011 cm^2 s^{-1}. In contrast, for a pure gold electrode the rate constant is 0.013 cm^2 s^{-1} for the same process. The question arises as to what will be the cyclic voltammetric response of the gold/modified graphite composite electrode?

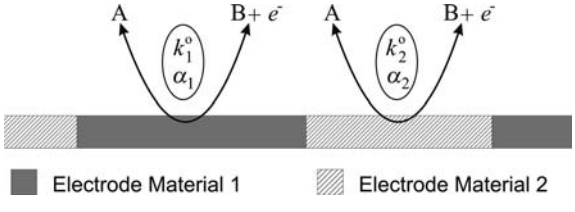

Fig. 16 An electrochemical reaction occurring on the same electrode surface with different Butler–Volmer characteristics at different spatial locations

Fig. 17 shows the cyclic voltammetric response of ferrocyanide at pure gold and pure anthraquinone-modified edge-plane pyrolytic-graphite electrodes; the difference in peak-to-peak potential separation, ΔE_{pp} reflects the different electrode kinetics identified above. We have simulated the response of the composite electrode for different scan rates and for different coverages ($0 \le \theta \le 1$) of gold on the graphite surface [2]. Figure 18 shows that ΔE_{pp} changes smoothly between the limits of pure gold and pure modified graphite but in a different fashion according to voltage scan rate. Figure 18 also shows a typical simulated voltammogram. The results in Fig. 18 can be used to estimate the coverage of gold from the measured values of ΔE_{pp} at different scan rates. The results are shown in Table 1 and may be compared with SEM images, from which a coverage of $\theta = 0.28$ was deduced. The excellent agreement with Table 1 is apparent [3]. It may be conclude that electrochemically heterogeneous electrodes can be simulated using the diffusion domain approximation.

Conclusions

The diffusion domain approximation is a powerful approach enabling accurate simulation of the voltammetric

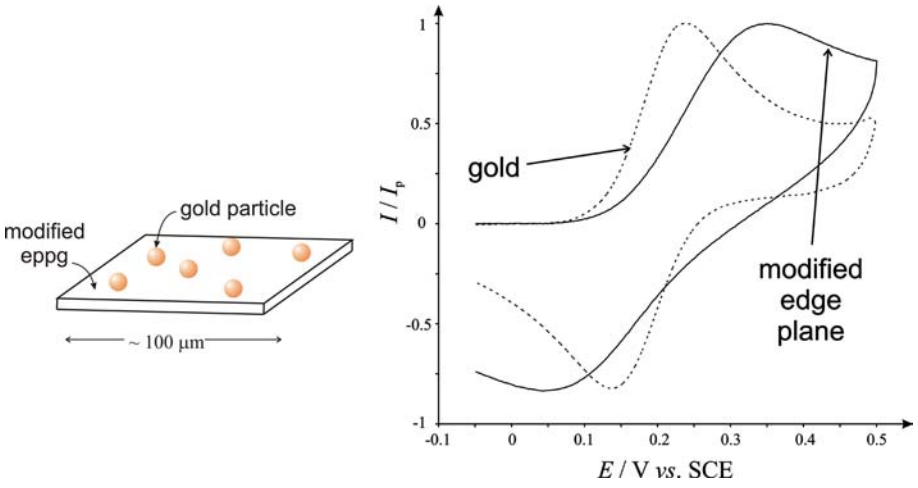

Fig. 17 Schematic diagram of the blocking gold particles on a modified edge-plane pyrolytic-graphite electrode (*left*) and the cyclic voltammetric response of aqueous ferrocyanide at pure gold and pure anthraquinone-modified edge-plane pyrolytic-graphite electrode (*right*)

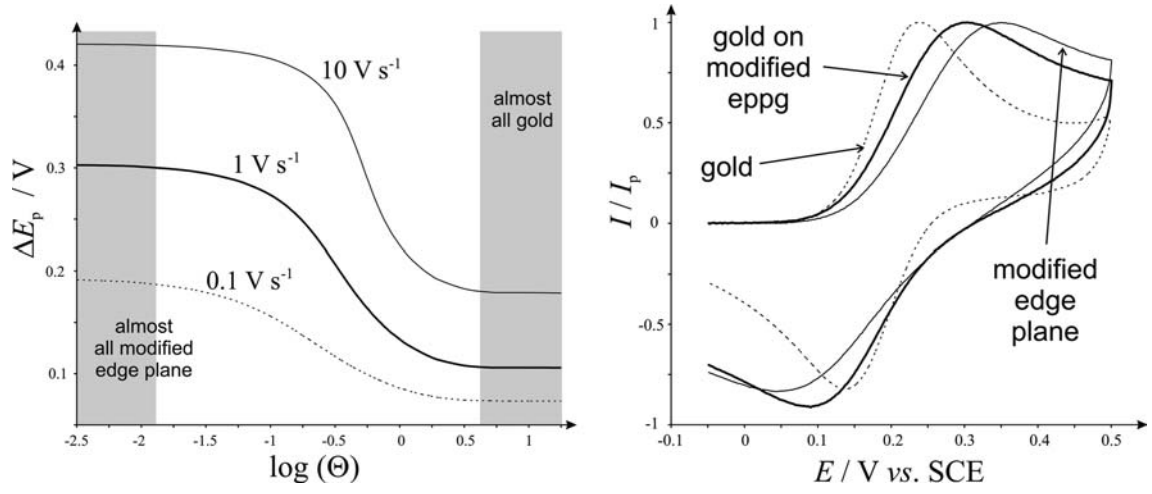

Fig. 18 Simulated working curves (*left*) showing the relationship between ΔE_p and log θ for cyclic voltammograms recorded at the gold particle anthraquinone-modified edge-plane pyrolytic-graphite electrode. Also shown (*right*) is a typical voltammetric response of gold on the modified edge-plane pyrolytic-graphite electrode with that of the bare gold and modified anthraquinone edge-plane electrode

Table 1 The measured peak-to-peak separation, ΔE_p, and inferred coverages, θ, of gold spheres on an edge-plane pyrolytic-graphite electrode

Scan rate, υ(V s^{-1})	ΔE_p(V)	θ
1.0	0.216	0.28
2.5	0.282	0.26
5.0	0.305	0.34
7.5	0.341	0.29
10.0	0.364	0.31

process at an electrochemically heterogeneous electrode. In particular the successful simulation of partially blocked electrodes, of microelectrode arrays, and of particle-modified (composite) electrodes is noted.

References

1. Brookes BA, Davies TJ, Fisher AC, Evans RG, Wilkins SJ, Yunus K, Wadhawan JD, Compton RG (2003) J Phys Chem B 107:1616
2. Davies TJ, Brookes BA, Fisher AC, Yunus K, Wilkins SJ, Greene PR, Wadhawan JD, Compton RG (2003) J Phys Chem B 107:6431
3. Chevallier FG, Davies TJ, Klymenko OV, Jiang L, Jones TGJ, Compton RG (2005) J Electroanal Chem 577:211
4. Davies TJ, Moore RR, Banks CE, Compton RG (2004) J Electroanal Chem 574:123
5. Amatore C, Saveant J-M, D Tessier (1983) J Electroanal Chem 147:39
6. Einstein A (1956) Investigation on the theory of the brownian movement. Dover Publications, New York
7. Davies TJ, Lowe ER, Wilkins SJ, Compton RG (2004) ChemPhysChem, In press
8. Banks CE, Davies TJ, Evans RG, Hignett G, Wain AJ, Lawrence NS, Wadhawan JD, Marken F, Compton RG (2003) Phys Chem Chem Phys 5:4053
9. Davies TJ, Brookes BA, Compton RG (2004) J Electroanal Chem 566:193
10. Davies TJ, Garner AC, Davies SG, Compton RG (2004) J Electroanal Chem 570:171
11. Wain AJ, Wadhawan JD, France RR, Compton RG (2004) Phys Chem Chem Phys 6:836

12. Wadhawan JD, Wain AJ, Compton RG (2003) ChemPhysChem 4:1211
13. Wadhawan JD, Wain AJ, Kirkham AN, Walton DJ, Wood B, France RR, Bull SD, Compton RG (2003) J Am Chem Soc 125:11418
14. Wain AJ, Wadhawan JD, Compton RG (2003) ChemPhysChem 4:974
15. Wain AJ, Lawrence NS, Greene PR, Wadhawan JD, Compton RG (2003) Phys Chem Chem Phys 5:1867
16. Chevallier FG, Davies TJ, Klymenko OV, Jiang L, Jones TGJ, Compton RG (2005) J Electroanal Chem, In press
17. Arrigan DWM (2004) Analyst 129:1157
18. Fletcher S, Horne MD (1999) Electrochem Commun 1:502
19. Grygar T, Marken F, Schroder U, Scholz F (2002) Collect Czech Chem Commun 67:163
20. Scholz F, Meyer B (1998) J Electroanal Chem 20:1